Effect of Temperature Variation on Remote Pressure Readout in Wirelessly Powered Intracranial Pressure Monitoring System

M. Waqas A. Khan, *Student Member, IEEE,* Muhammad Rizwan, *Student Member, IEEE,* Lauri Sydänheimo, *Member, IEEE,* Yahya Rahmat-Samii, *Fellow, IEEE,* Leena Ukkonen, *Member, IEEE,* Toni Björninen, *Member, IEEE*

***Abstract*—An implantable pressure monitoring system is a compelling approach to home monitoring of intracranial pressure in the long term. In our approach, an on-body unit powers a cranially concealed system where a piezoresistive element senses the pressure. A data transmission unit built in the same platform emits a signal at a pressure dependent frequency through a miniature far field antenna. In this work, we focus on assessing the impact of variable temperature on the pressure readout at an off-body unit through in-vitro experiments.**

I. Introduction

The cerebral blood flow (CBF) must meet the high metabolic needs of the brain to sustain regular neurological functions and life. Cerebral perfusion pressure (CPP) is the pressure gradient between arteries and veins that causes blood flow into the brain. It is commonly estimated as the difference between the mean arterial pressure (MAP) and intracranial pressure (ICP) [1] so that

$$\mathrm{CBF} = \frac{\mathrm{CPP}}{\mathrm{CVR}} = \frac{\mathrm{MAP} - \mathrm{ICP}}{\mathrm{CVR}}, \qquad (1)$$

where CVR is the cerebrovascular resistance. ICP depends on hydrodynamic and hemodynamic parameters controlled by complex and interlinked physico-chemical mechanisms [2–3], whereas cerebrovascular autoregulation stabilises CBF over a broad range of CPP by modifying CVR primarily by the constriction or dilation of cerebral arteries [4].

In adults, ICP is normally 7–15 mmHg (supine position) [5]. Since the cranial cavity is a fixed space with three components: blood, CSF and brain, an abnormal volume-increase in any of them may lead to raised ICP and consequently reduced CBF, as defined in equation (1). This happens when the autoregulation dysfunctions or meets its compensatory limits due to mass lesion, oedema or otherwise disturbed CSF formation-reabsorption balance, for instance. Raised ICP and reduced CBF are both pathological [1,3,5–6]. In particular, reduced CBF causes ischemia and infarction. Thus, the monitoring and management of ICP are frequent and life-saving procedures.

In critically ill patients, the common clinical practice for monitoring of ICP is the insertion of a catheter in the ventricular system of the brain through a burr hole (ventriculostomy) [5–6]. This method is accurate, allows on-site recalibration as well as drainage of CSF to manage raised ICP, but due to its invasiveness, an array of non-invasive alternatives are available for in-hospital use [5]. However, people who are predisposed to disturbed CSF flow or formation-reabsorption balance due to neurological malformations or a previous neurocritical event, for instance, would greatly benefit from home monitoring of ICP. To address the need, scientists are developing technology for wireless implantable sensors to enable safe and reliable home monitoring of ICP in long-term. Several recent studies reviewed below provide views on the balance between device size, energy consumption, and functionality in the current state-of-the-art.

Authors of [7] sealed an antenna and electronics in a transcranial cylinder and demonstrated the wireless monitoring of subdural pressure in-vivo. To minimize invasiveness, authors of [8–9] studied miniature coils loaded with capacitive MEMS pressure sensors. These devices are battery-free, small and flexible, but due to passive operation, are limited in functionality and readout distance. As an alternative, the authors of [10] investigated a wirelessly powered battery-free system where a supercapacitor served as temporary energy storage to supply active electronics. Here the coils for inductive powering at a low frequency of 180 kHz dominated the device size. Authors of [11] presented a battery-free wireless sensing system comprising piezoresistive element, active electronics, coil for inductive powering (at 15 MHz), and a miniature antenna for data transmission on a thin and flexible platform. The system was capable of transmitting the pressure data to a receiver at a distance of one metre in in-vitro experiments. Finally, authors of [12] have demonstrated a millimetre-scale pressure-to-digital microsystem targeted for ICP monitoring applications, which consumed only 130 nW at 60-Hz sampling rate.

In this work, we study the impact of variable temperature on the pressure readout from the wireless pressure monitoring system based on a piezoresistive element that we have presented in our previous work [11]. This investigation is motivated by the fact that the temperature changes influences these types of sensors through the thermal expansion of the diaphragm, for instance [13–14].

II. Overview of the Pressure Sensing System

Fig. 1(a) presents an overview of the functional blocks of the system. The on-body unit consists of a 2-turns loop (outer

This research was funded by Academy of Finland, Jane and Aatos Erkko Foundation, and TEKES.

M. W. A. Khan, M. Rizwan, L. Sydänheimo, L. Ukkonen and T. Björninen are with BioMediTech Institute and Faculty of Biomedical Sciences and Engineering, Tampere University of Technology, Tampere, Finland (e-mail: {muhammad.khan, muhammad.rizwan, lauri.sydanheimo, leena.ukkonen, toni.bjorninen}@tut.fi).

Y. Rahmat-Samii is with the Department of Electrical Engineering, University of California, Los Angeles, Los Angeles, CA 90095 USA (email: rahmat@ee.ucla.edu).

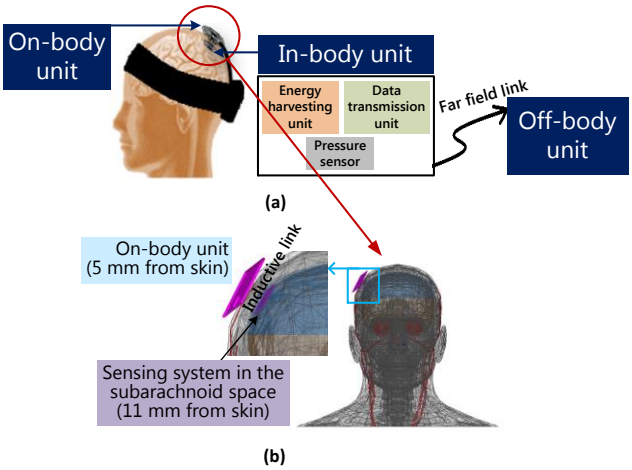

Fig. 1. (a) Functional bocks of the wireless ICP monitoring system. (b) Anatomical model used in the electromagnetic modelling of the inductive power link between the on-body unit and the sensing system.

diameter: 32.1 mm) [15], an impedance matching circuit and a power source. It energises the pressure sensor through inductive coupling at 15 MHz. The pressure sensor picks up the energy through a two-turns loop (13.5 mm × 12.9 mm). A miniaturised far field antenna (6 mm × 5 mm) placed (along with other electronics) in the empty space in the centre of the loop conveys the pressure data directly to an off-body unit reducing the hardware complexity in the on-body unit

We used ANSYS HFSS v15 (full-wave electromagnetic field solver based on the finite element method) in modelling of the antennas and wireless performance of the system in biological operation environment. As indicated in Fig. 1(b), we employed an anatomical model to optimise the power efficiency of the inductive link, as this is a crucial factor for the operation of the system. Fig. 2 shows the modelling outcome, which predicts that a relatively high link power efficiency of −4.1 dB could be achieved at 15 MHz. This is within 1 dB from the value obtained in air in the absence of the body tissue. For more details of the optimisation of inductive link and the miniature far field antenna, we refer to our previous works [15–16] and [17], respectively. Finally, in the experiment, which we will report in the next Section, we have used a half-wavelength dipole connected to a spectrum analyser to capture the sensor's transmission in the 2.4 GHz industrial, scientific and medical (IMS) radio band.

In addition to antennas, the in-body unit integrates electronics to produce DC voltage that supplies the

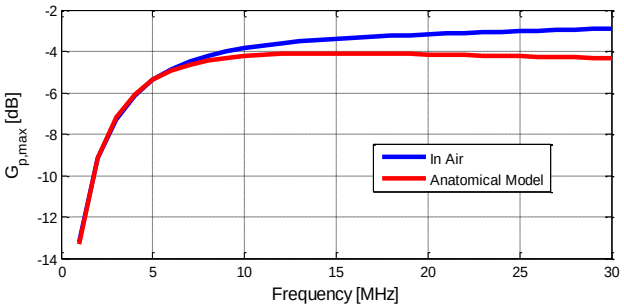

Fig. 2. Simulated link power efficiency of the optimised inductive link.

piezoresistive sensor and the components in the data transmission unit that are all listed in Fig. 3 at approximately three volts. The output DC voltage of the sensor drives a voltage-controlled oscillator in the data transmission unit to map the pressure value to the frequency of transmission. As indicated in Fig. 1(b), the sensor is in the subarachnoid space and thus it senses ICP directly from the pressure in the CSF. We covered the whole in-body unit (except for the sensor's pressure aperture) in biocompatible MED-2000 silicone adhesive material. The coated system had the overall thickness of approximately one millimetre. Finally, we coated the whole system (including the sensor's pressure aperture) with 2-µm layer of Parylene C to achieve a pinhole free coating.

III. Measurement and Discussion

Fig. 4 shows the complete measurement setup we used in the wireless testing and the manufactured in-body unit, on-body two-turns loop and the half-wavelength dipole. We impedance-matched the two-turns loop of the in-body unit to the rectifier with a single shunt capacitor. A capacitor in series with the antenna and inductor in parallel were used in the on-body two-turns loop. The measured S-parameters of the inductive link were: $S_{11} = -5.3$ dB, $S_{22} = -7.3$ dB and $S_{21} = -15.5$ dB as reported in Fig. 3.

In the experiment, we immersed the pressure sensor in liquid that mimicked the dielectric properties of human head. The liquid was mixed from water, sugar and salt as explained in [17] to achieve the relative permittivity and loss tangent of $\varepsilon_r = 39.2$ and $\sigma = 1.8$ S/m at 2.45 GHz. Moreover, we used a heating plate to control the temperature of the liquid and set distance between the in-body and on-body units to 16 mm as it was in the simulation of the inductive link. Finally, we connected an automated pressure calibrator ADT761 through a tube to the bottle to control the pressure in it. The half-wave-

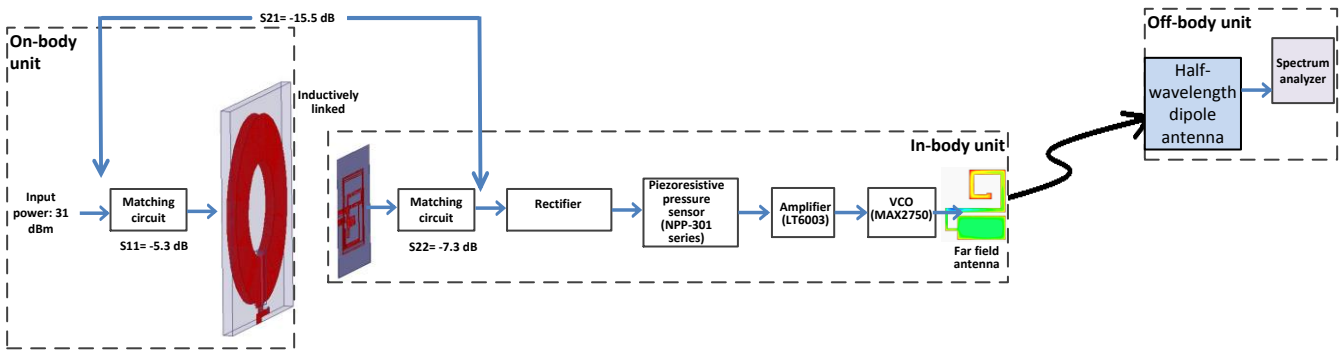

Fig. 3. Measured S-parametres and power transfer to the sensing system.

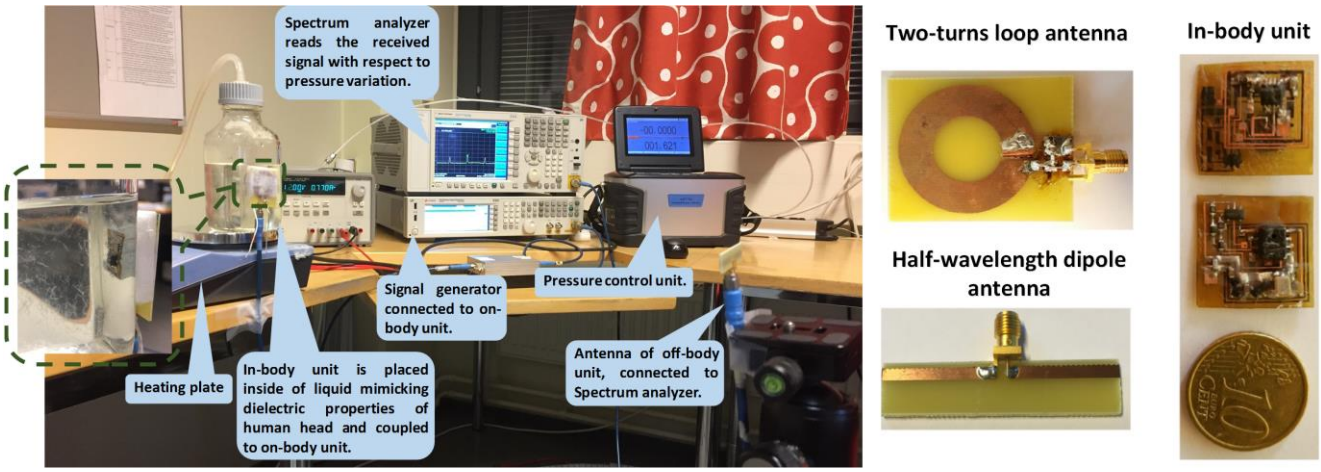

Fig. 4. The measurement setup for wireless testing and the manufactured in-body unit, on-body two-turns loop, and the half-wavelength dipole.

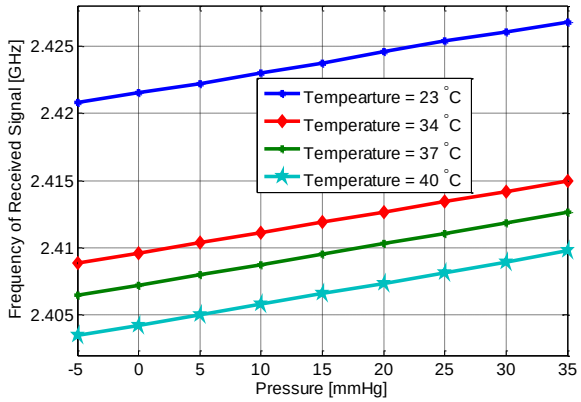

Fig. 5. Measured sensor's transmission frequency versus pressure in different temperatures.

length dipole antenna was at a distance of one metre from the in-body unit in polarisation-matched configuration for capturing the sensor's signal. To energise the sensor, we fed the on-body two-turns loop to with 31 dBm, which, according to our earlier investigations, is within the limits of human safety in terms of exposure to electromagnetic fields at the frequency of 15 MHz [11]. As indicated in Fig. 3, this provided 15.5 dBm of power to the in-body unit and activated the sensor fully in the experiment.

To obtain the relationship between the pressure and sensor's signal frequency we tracked the frequency with spectrum analyser as we increased the pressure from −5 mmHg to 35 mmHg. The studied pressure range was selected to cover hypotensive (below 7 mmHg), regular and hypertensive (above 15 mmHg) ICP with a maximum that is well above the clinical threshold of 20 mmHg [6] for starting ICP lowering treatments. To assess the impact of temperature variation, we repeated the experiment in four different temperatures: 23 °C, 34 °C, 37 °C, and 40°C.

Fig. 5 presents the results from the experiment. They show that in all temperatures, the frequency-pressure relation follows a linear model. There was a total shift of 6 MHz, 6.15 MHz, 6.2 MHz and 6.3 MHz in frequency of the sensor's signal corresponding to 40 mmHg change in pressure at 23 °C, 34 °C, 37 °C and 40 °C respectively. This indicates that temperature variation has negligible effect on the slope of pressure-frequency graphs, i.e. the increase in temperature resulted only in a downwards level-shift. On average, the shift was 0.953 MHz per 1 °C. This translates to a deviation of 7 mmHg in the pressure readout due to a change of 1°C in the temperature. Relative to the range of normal ICP variations, this is a notable variability and thus raises the need for temperature compensation to guarantee reliable pressure readout. Possible means include measuring the temperature separately and compensating the error at the off-body unit or adding a temperature sensor in the in-body unit itself.

IV. Conclusion

We studied the impact of temperature variation on the pressure readout of an inductively powered intracranial pressure monitoring system based on a piezoresistive element. Our experimental results at four different temperatures (23 °C, 34 °C, 37 °C and 40 °C) predicted an average error of 7 mmHg due to 1 °C change in temperature. We found that this was only due to a level shift in the sensor's linear transmission frequency versus pressure graphs. This means that a simple temperature measurement may be applicable in removing the impact of temperature variations from the pressure readout at the off-body unit.

References

[1] M. Czosnyka and J. D. Pickard, "Monitoring and interpretation of intracranial pressure," *J. Neurol., Neurosurg. Psychiatry*, vol. 75, no. 6, pp. 813–821, Jan 2004.

[2] X. Hu, V. Nenov, M. Bergsneider, T. C. Glenn, P. Vespa, N. Martin, "Estimation of hidden state variable of the intracranial system using constrained nonlinear Kalman filters," *IEEE Trans. Biomed. Eng.*, vol. 54, no. 4, pp. 597–610, Apr. 2007.

[3] C. E. Johanson, J. A. Duncan, P. M. Klinge, T. Brinker, E. G. Stopa, G. D. Silverberg, "Multiplicity of cerebrospinal fluid functions: New challenges in health and disease," *J. Cerebrospinal Fluid Res.*, vol. 5, no. 10, 32 pages, May 2008.

[4] M. J. Cipolla. "Control of cerebral blood flow," in *The Cerebral Circulation*. Morgan & Claypool Life Sciences, 2009. Available from: https://www.ncbi.nlm.nih.gov/books/NBK53082/

[5] L. A. Steiner, P. J. D. Adnrews, "Monitoring the injured brain: ICP and CBF," *Br. J. Anesth.*, vol. 97, no. 1, pp. 26–38, May 2006.

[6] P. H. Raboel, J. Bartek., M. Andresen, B. M. Bellander, and B. Romner, "Intracranial pressure monitoring: invasive versus non-invasive methods – a review," *Crit. Care Res. Pract.*, vol. 2012, Article ID: 950393, 14 pages, Mar. 2012.

[7] U. Kawoos, M.-R. Tofighi, R. Warty, F. A. Kralick, A. Rosen, "In-vitro and in-vivo trans-scalp evaluation of an intracranial pressure implant at 2.4 GHz," *IEEE Trans. Microw. Theory Techn.*, nol. 56, no. 10, pp. 2356–2365, Oct. 2008.

[8] L. Y. Chen, B. C. K. Tee, Z. Bao, et al., "Continuous wireless pressure monitoring and mapping with ultra-small passive sensors for health monitoring and critical care," *Nature Commun.*, vol. 5, article 5028, Oct. 2014.

[9] Mohammad H. Behfar, E. Moradi, T. Björninen, L. Sydänheimo, L. Ukkonen, "Biotelemetric wireless intracranial pressure monitoring: an in vitro study," *Intl. J. Antennas and Propag.*, vol. 2015, article ID 918698, 10 pages, Nov. 2015.

[10] P. Hu, Y. W. You, F. Y. B. Chen, D. McCormick, D. M. Budgett, "Wireless power supply for ICP devices with hybrid supercapacitor and battery storage," *IEEE J. Emerg. Sel. Topics Power Electron.*, vol. 4, no. 1, pp. 273–279, Mar. 2016.

[11] M. W. A. Khan, L. Sydänheimo, L. Ukkonen, T. Björninen, "Inductively powered pressure sensing system integrating a far-field data transmitter for monitoring of intracranial pressure," *IEEE Sensors J.*, vol. 17, no. 7, pp. 2191–2197, Apr. 2017.

[12] M. M. Ghanbari, J. M. Tsai, A. Nirmalathas, R. Muller, S. Gambini, "An energy-efficient miniaturized intracranial monitoring system," *IEEE J. Solid-State Circuits*, vol. 52, no. 3, pp. 730–734, Mar. 2017.

[13] S.-C. Kim, K. D. Wise, W.-K. Chen, "Temperature sensitivity in silicon piezoresistive pressure transducers," *IEEE Trans. Electron. Dev.*, vol. 30, no. 7, pp. 802–810, July 1983.

[14] U. Aljancic, D. Resnik, D. Vrtacnik, M. Mozek, S. Amon, "Temperature effects modeling in silicon piezoresistive pressure sensor," *IEEE Mediterranean Electrotechnical Conference*, pp. 36–40, 2002.

[15] M. W. A. Khan, T. Björninen, L. Sydänheimo, and L. Ukkonen, "Remotely powered piezoresistive pressure sensor: toward wireless monitoring of intracranial pressure," *IEEE Microw. Wireless Compon. Lett.*, vol. 26, no. 7, pp. 549–551, June 2016.

[16] M. W. A. Khan, T. Björninen, L. Sydänheimo, L. Ukkonen, "Characterization of two-turns external loop antenna with magnetic core for efficient wireless powering of cortical implants," *IEEE Antennas Wireless Propag. Lett.*, vol. 15, pp. 1410–1413, June 2016.

[17] M. W. A. Khan, E. Moradi, L. Sydänheimo, T. Björninen, Y. Rahmat-Samii, L. Ukkonen, "Miniature co-planar implantable antenna on thin and flexible platform for fully wireless intracranial pressure monitoring system," *Intl. J. Antennas Propag.*, Article ID: 9161083, 9 pages, Jan. 2017.